BNL-61380

JOURNAL OF GEOPHYSICAL RESEARCH, VOL. 100, NO. D4, PAGES 7263–7273, APRIL 20, 1995

Peroxy radical concentration and ozone formation rate at a rural site in the southeastern United States

Lawrence Kleinman, Yin-Nan Lee, Stephen R. Springston, Jai H. Lee, Linda Nunnermacker, Judith Weinstein-Lloyd,[1] Xianliang Zhou, and Leonard Newman

Department of Applied Science, Environmental Chemistry Division, Brookhaven National Laboratory, Upton, New York

Abstract. As part of the Southern Oxidants Study, Brookhaven National Laboratory operated an intensive measurement site near Metter, Georgia, during parts of the summers of 1991 and 1992. Measurements were made of photochemically active trace gases and meteorological parameters relevant to determining causes for elevated ambient ozone concentration. The 1992 data set was used to calculate peroxy radical concentration and ozone formation rate based on determining the departure from the photostationary state (PSS) and based on a radical budget equation, such as applied previously to the 1991 data set. Averaged over the 28-day experimental period, we find maximum radical production occurring near noon at 2.5 ppb h^{-1}, maximum peroxy radical concentration also occurring near noon at 80 ppt, and maximum ozone production of 8 ppb h^{-1} occurring near 1000 EST. Ozone photolysis accounts for 55% of radical production, HCHO and other carbonyl compounds about 40%. The radical budget and PSS methods depend in different ways on atmospheric photochemistry and a comparison between them affords a test of our understanding of the photochemical production of O_3. We find that these methods agree to the extent expected based on uncertainty estimates. For the data set as a whole, the median estimate for fractional error in hourly average peroxy radical concentration determined from the radical budget method is approximately 30% and from the PSS method, 50%. Error estimates for the PSS method are highly variable, becoming infinite as peroxy radical concentration approaches zero. This behavior can be traced back to the difference form of the PSS equations. To conduct a meaningful comparison between the methods, the data set was segregated into subsets based on PSS uncertainty estimates. For the low-uncertainty subset, consisting of a third of the whole data set, we find that the ratio of peroxy radical concentration predicted from the PSS method to that predicted from the radical budget method to be 1.22 ± 32%.

1. Introduction

The Southern Oxidants Study (SOS) [*University Corporation for Atmospheric Research* (*UCAR*), 1990] was initiated for the purpose of understanding the pervasive high levels of O_3 observed in the southeastern United States [*Meagher et al.*, 1987; *Aneja et al.*, 1990; *National Research Council* (*NRC*), 1991]. As part of this study, Brookhaven National Laboratory operated a "SENIOR" (South Eastern Network for Intensive Oxidant Research) measurement site on a campaign basis during parts of the summers of 1991 and 1992. An extensive suite of photochemical trace gas and meteorological observations directed at determining the relations between oxidants and their precursors was obtained in both years.

In this study we are concerned with the prediction of O_3 formation rates and peroxy radical concentrations based on a radical budget calculation and based on the photostationary state (PSS) relations. We compare these two approaches using data from the 1992 campaign. In a previous study using the 1991 data set, the radical budget approach was used to determine production rates for O_3 which were then compared with other trace gas measurements [*Kleinman et al.*, 1994a]. We will refer to the 1991 study as "SOS91."

Estimates of peroxy radical concentration and O_3 formation rate have been obtained for a diverse range of locations via the use of the PSS equations [*Parrish et al.*, 1986; *Chameides et al.*, 1990; *Ridley et al.*, 1992; *Davis et al.*, 1993; *Cantrell et al.*, 1993; *Bawkin et al.*, 1994; *Poulida et al.*, 1994]. Diurnal cycles of peroxy radical concentration and their relation to other atmospheric variables such as NO_x($NO + NO_2$) concentration and solar UV have been discussed. Several studies including those at Mauna Loa [*Ridley et al.*, 1992] and at the Rural Oxidants in the Southern Environment (ROSE) site in rural Alabama [*Cantrell et al.*, 1993] have shown good agreement between PSS-derived peroxy radical concentrations and results from detailed photochemical models.

The radical budget approach for calculating O_3 formation rates has, to the best of our knowledge, only been applied to

[1] Also at Chemistry/Physics Department, State University of New York/Old Westbury.

Copyright 1995 by the American Geophysical Union.

Paper number 95JD00215.
0148-0227/95/95JD-00215$05.00

the 1991 SOS campaign. Similar equations, however, have been used to determine the qualitative dependence of O_3 production on precursor concentration [*Sillman et al.*, 1990] and the dependence of peroxide concentration on radical production rates [*Kleinman*, 1986, 1991]. These qualitative predictions appear to be in accord with observations [*Daum et al.*, 1990] and detailed calculations [*McKeen et al.*, 1991].

Radical budget and PSS calculations require different combinations of atmospheric observations and depend on different features of the atmospheric photochemical system. An important component of the present study is a comparison between these two techniques. We rely on the statistical tests used by *Cantrell et al.* [1993] in their comparison between peroxy radical concentration derived from the PSS equations and that measured with a chemical amplifier. The correspondence between PSS and radical budget predictions is compared to that expected based on the uncertainty estimates for each technique.

We conclude with a comparison between observed and calculated diurnal cycles for O_3. This comparison yields information on transport and deposition as the calculations depend only on chemistry, whereas the observations also reflect the influence of transport and deposition.

2. Experiment

The measurement site operated by Brookhaven National Laboratory (BNL) was located in a cleared area inside of George L. Smith State Park (32°32′N, 82°08′W), Candler County, approximately 110 km WNW of Savannah, Georgia. This is the same site as used in the 1991 campaign and is described in detail in SOS91. Here we briefly note that the location is forested and that it is remote from major emission sources. As before, we refer to this site as the Metter site after the name of a nearby city.

Instrumentation at Metter in 1992 was similar to that in 1991. Measurements include O_3, NO, NO_2, HNO_3 (including particulate nitrate), NO_y (as determined by a chemiluminescence NO detector preceded by a Mo convertor operated at 350°C), PAN, SO_2, HCHO, other carbonyls (acetaldehyde, acetone, glycolaldehyde, glyoxal, and methylglyoxal) organic acids (glyoxylic and pyruvic), H_2O_2, organic peroxides (hydroxymethylhydroperoxide and comeasured analogs and methylhydroperoxide and comeasured analogs), CO, NMHC (performed by Georgia Institute of Technology), solar UV, b_{scat}, wind speed and direction, temperature, and dew point. Sampling was done at a height of 3 to 4 m above the ground. An overview of the instrumentation is contained in SOS91. Further details on the measurement of peroxides can be found in the work of *Lee et al.* [1993, 1994]; the measurements of carbonyl compounds are described by *Lee and Zhou* [1993] and *Lee et al.* [1994].

A significant improvement was made in 1992 to the NO_x detector by decreasing the residence time in the gas inlet system. Revised estimates for the uncertainty in NO and NO_2 determinations are ±10 and ±20%, respectively. In 1992, pyruvic and glyoxylic acids were added to the list of measured compounds. The sampling frequencies for carbonyl compounds and peroxides was greater than in 1991. Continuous or near-continuous (greater than 90%) coverage was obtained for many quantities, including all meteorological parameters, b_{scat}, and the concentrations of O_3, NO, NO_2, HNO_3, NO_y, SO_2, and CO.

3. Results

Measurements were made over a 28-day period between June 1 and June 28, 1992. This period was cooler and dryer than the 1991 intensive held in July and August. Average daily maximums and minimums for temperature were 29.5° and 19.2°C and for dew point 21.2° and 17.4°C. Ozone concentrations were slightly higher in 1992 with an average daily maximum value of 53 ppb as compared with 48 ppb in 1991.

Of particular interest in this study are the species and parameters that determine the chemical rate of production of O_3. According to the radical budget approach (SOS91), O_3 formation rates can be specified in terms of radical precursor concentration, photolysis rate constants, and NO concentration. The PSS equations give O_3 production rates in terms of O_3, NO, NO_2, and j_{NO_2} (the photolysis rate constant for NO_2). A portion of the data that will be used for these calculations is shown in Figures 1 and 2, which depict diurnal cycles for hourly averaged values of O_3, HCHO, NO, NO_2, and solar intensity.

As in SOS91, we have split the measurement period into three subsets; low-O_3 days, mid-O_3 days, and high-O_3 days. The maximum hourly average O_3 concentration on a given day determines the subset to which that day belongs. Twenty five percent of the days were called high O_3, 50% middle, and the remaining 25% low. Figures 1 and 2 show diurnal cycles for the three subsets as one way of visualizing variability during the experimental period.

Five hours of data have been removed from the NO and NO_2 data set and the calculations that follow due to the occurrence of very high plumelike NO_x concentrations. Many smaller plumelike features occur at night and are evident in the NO record in Figure 1c, even though the diurnal cycles in this figure are averaged over multiday periods. The extent to which these features contribute to an average nonzero nighttime NO concentration is surprising in view of the rapid reaction between NO and O_3. Figure 3 shows hourly average NO concentration between midnight and 0400 EST as a function of O_3. The high NO observations occur only at low or near-zero O_3 concentration. It appears that there is a competition between surface or near-surface emissions (i.e., soil or motor vehicles) and reaction of NO with O_3, resulting in residual NO. Nonzero nighttime NO concentrations, averaging 60 ppt at 8-m elevation, have been observed at a similar rural southeastern U.S. site by *Poulida et al.* [1994].

4. Peroxy Radical Concentration and Ozone Productions

On the basis of the data collected at Metter, there are two ways of determining peroxy radical concentration and production rates for O_3. These are the radical budget and PSS methods. In this section these methods are described and applied to the Metter data set. We compare results from these two methods and also compare predictions of the chemical contribution to the time rate of change of O_3 with O_3 observations.

4.1. Radical Budget

In situ chemical production rates of O_3 were calculated from a radical budget equation using measured values of NO and radical precursors. Our approach is the same as in

SOS91. The implementation is improved due to improvements in the NO_x detector, measurement of additional carbonyl compounds, and an increased frequency of HCHO, peroxide, and carbonyl measurements.

Radicals are formed in the lower troposphere by a variety of processes, the most important of which are thought to be the photolysis reactions of O_3 and HCHO.

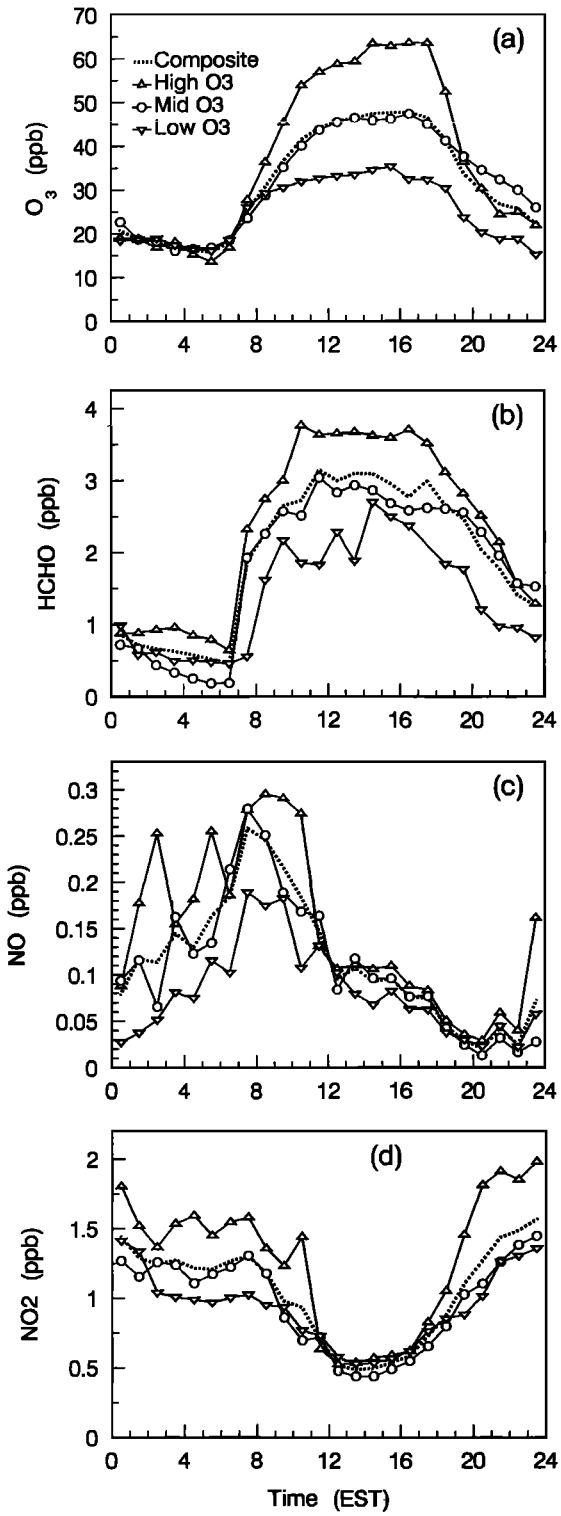

Figure 1. Diurnal cycles for (a) O_3, (b) HCHO, (c) NO, and (d) NO_2 for the whole experimental period and for the high-, mid-, and low-O_3 day subsets, as defined in the text.

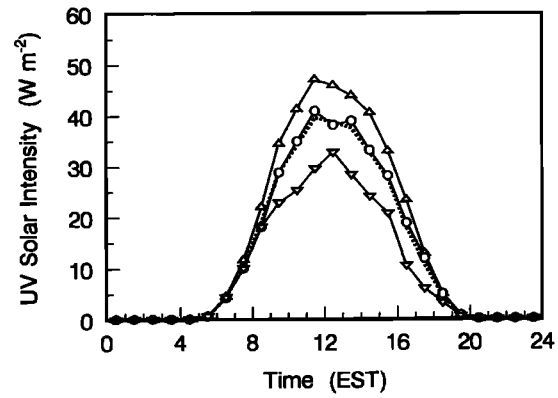

Figure 2. Diurnal cycle for UV solar intensity for the whole experimental period and for the high-, mid-, and low-O_3 day subsets. Curve symbols are the same as in Figure 1.

(R1) $O_3 + h\nu \rightarrow O(^1D)$

(R2) $O(^1D) + M \rightarrow O(^3P)$

(R3) $O(^1D) + H_2O \rightarrow 2OH$

(R4) $HCHO + h\nu \rightarrow CO + 2HO_2$

The total radical formation rate, Q, as calculated from SOS data, also contains contributions from the photolysis of other carbonyl compounds and peroxides:

$$Q = 2J_1k_3[H_2O][O_3]/(k_3[H_2O] + k_2[M]) + 2J_4[HCHO] + \sum 2J_i[\text{carbonyl}(i)] + \sum J_i[\text{peroxide}(i)] \quad (1)$$

where k is the reaction rate constant and J is the photolysis rate constant for the similarly labeled reactions.

There are three major categories of radical removal reactions: reactions involving NO_x, such as $OH + NO_2 \rightarrow HNO_3$, bimolecular destruction processes such as $OH + HO_2 \rightarrow H_2O + O_2$, and peroxy radical combination reactions

(R5) $2HO_2 \rightarrow H_2O_2$

(R6) $HO_2 + RO_2 \rightarrow ROOH$

Sources and sinks of free radicals must be in balance. As before, we take advantage of the circumstance that under the low NO_x conditions that prevail in rural Georgia, radical destruction occurs predominately by peroxide formation. The balance equation for free radicals becomes

$$Q = 2k_5[HO_2]^2 + 2k_6[HO_2][RO_2] \quad (2)$$

which can be solved for the total peroxy radical concentration if the relative proportions of HO_2 and RO_2 are known. If $[RO_2]/([HO_2] + [RO_2]) = \alpha$, then

$$[HO_2] + [RO_2] = Q^{1/2}/(2k_{\text{eff}})^{1/2} \quad (3a)$$

where

$$k_{\text{eff}} = k_5(1 - \alpha)^2 + k_6(1 - \alpha)\alpha \quad (3b)$$

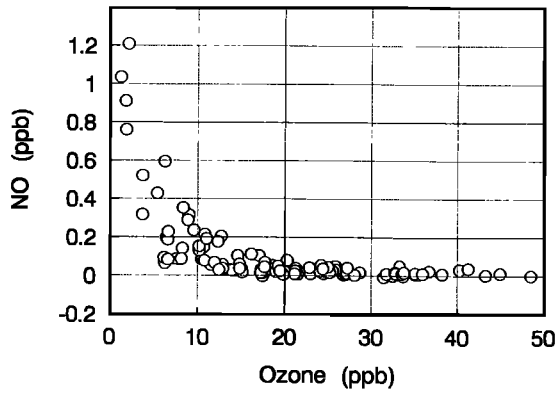

Figure 3. Hourly average measurements of NO as a function of coincident O_3 between midnight and 0400 EST.

The total peroxy radical concentration is used to calculate an O_3 formation rate according to the following sequence of reactions:

(R7) $HO_2 + NO \rightarrow NO_2$

(R8) $RO_2 + NO \rightarrow NO_2$

followed with nearly 100% yield by the rapid reactions

(R9) $NO_2 + h\nu \rightarrow NO + O$

(R10) $O + O_2 \rightarrow O_3$

yielding

$$dO_3/dt(+) = k_7[HO_2][NO] + k_8[RO_2][NO],$$

$$\approx k_7([HO_2] + [RO_2])[NO] \quad (4)$$

where $k_7 \approx k_8$ and the "plus" sign indicates that only production terms are included in the time rate of change. Combining (3) and (4) yields the following expression for O_3 formation in terms of observed concentrations, known rate constants, and the parameter α which is estimated based on model calculations performed for similar regions [*Trainer et al.*, 1987, 1991]:

$$dO_3/dt(+) = k_7 Q^{1/2}/(2k_{eff})^{1/2}[NO] \quad (5)$$

Major chemical loss pathways for O_3 are photolysis (equations (R1)–(R3)) and reaction with HO_2:

(R11) $HO_2 + O_3 \rightarrow 2O_2 + OH$

The total chemical rate of change of O_3, taking into account these loss processes, is

$$dO_3/dt = dO_3/dt(+) - \text{Loss} \quad (6)$$

where

$$\text{Loss} = J_1 k_3[H_2O][O_3]/(k_3[H_2O] + k_2[M]) + k_{11}[HO_2][O_3] \quad (7)$$

Radical budget quantities were calculated with 1-hour time resolution using hourly averaged values of solar intensity, temperature, dew point, and the concentrations of O_3, NO, peroxides, and carbonyls. This time resolution is dictated by the 1-hour sampling times for HCHO and other carbonyl compounds. Missing data were dealt with in one of several ways depending on the importance to the final calculations. An interpolation procedure was used to fill in missing HCHO values for gaps up to 3 hours in duration. For the other carbonyl compounds and for peroxides, average values for the appropriate time of day and data subset (i.e., high, middle, and low) were used to fill in for missing data points. The data set for O_3, temperature, and dew point was complete for all daylight hours of the 28-day experimental period. A missing value for HCHO (after the interpolation procedure) or a missing value for solar intensity prevented the calculation of peroxy radical concentration for that hour. Missing values for NO, solar intensity, or HCHO prevented the calculation of $dO_3/dt(+)$. Calculated quantities are then averaged over the appropriate days constituting high, middle, and low O_3 subsets.

The effective rate constant for the peroxy radical combination, k_{eff}, was determined based on a value of 0.65 for α (as appropriate for a forested region [*Trainer et al.*, 1987, 1991], $k_5 = 5.4 \times 10^{-12}$, and $k_6 = 6 \times 10^{-12}$ [*Stockwell et al.*, 1990].

Photolysis rate constants were calculated from Eppley radiometer measurements of solar UV using the radiative transfer code of *Madronich* [1987] and the methods outlined in SOS91. In brief, the radiative transfer model was used to calculate photolysis rate constants for clear sky conditions taking into account the climatological O_3 column and aerosol optical depth, time of day and month, and location of the sampling site. Radiometer readings were used to correct for variable cloud cover by multiplying the calculated photolysis rate constants by the ratio of measured solar UV on a given day to that measured at the same time of day on a day without clouds.

An estimate of the uncertainty in hourly average peroxy radical concentration and $dO_3/dt(+)$ follows from the estimated uncertainties in Q, k_{eff}, and NO. We assume the following independent component uncertainties: $\sigma_1(Q) = 0.25Q$ for the relation between irradiance and actinic flux; $\sigma_2(Q) = 0.2Q$ for uncertainties in measuring radical precursor concentrations and calculating dissociation rate constants from actinic flux; $\sigma(NO) = 0.1[NO]$; and $\sigma(k_{eff}) = 0.53k_{eff}$ from an assumed uncertainty of 0.15 in α and 3×10^{-12} in k_6. Errors are propagated according to

$$\sigma(f)_{total} = \left(\sum (\sigma_i \partial f/\partial x_i)^2\right)^{1/2} \quad (8)$$

yielding fractional uncertainties (i.e., $\sigma(f)_{total}/f$) for $[HO_2] + [RO_2]$ and $dO_3/dt(+)$ of 31 and 33%, respectively. In contrast to SOS91, errors in $dO_3/dt(+)$ are no longer dominated by uncertainties in measuring NO but rather by uncertainties in k_{eff}.

Figure 4 shows diurnal cycles of radical production rate for high-, mid-, and low-O_3 days calculated from (1) following these procedures. A partial breakdown according to precursor species is given in Table 1 and Figure 5 for high-O_3 days. The importance of radical precursors other than O_3 is evident. Peroxy radical concentrations from (3) and O_3 chemical formation rates from (4) are given in Figures 6 and 7, respectively. Net chemical change rates are shown later on in comparison with observed hour-to-hour O_3 changes. Figures 4, 6, and 7 indicate that radical production, peroxy radical concentration, and O_3 formation rate occur in the

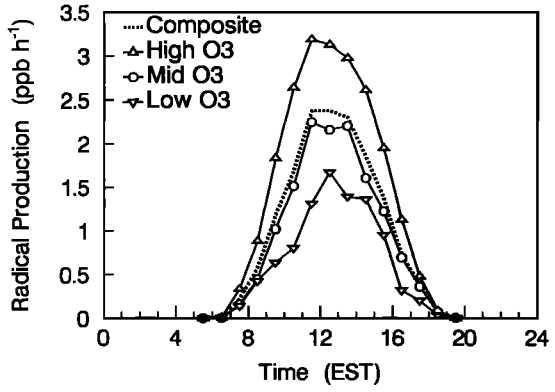

Figure 4. Diurnal cycle for radical production rate calculated according to equation (1) for the whole experimental period and for the high-, mid-, and low-O_3 day subsets. Curve symbols are the same as in Figure 1.

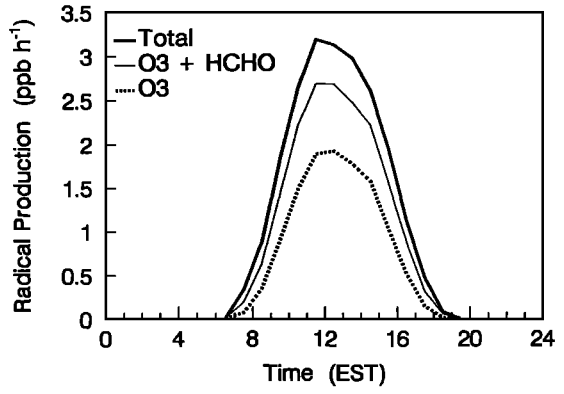

Figure 5. Diurnal cycle for radical production rate on high O_3 days, by species. Compounds contributing to the other carbonyl category are acetaldehyde, acetone, glyoxal, glycolaldehyde, and methylglyoxal. The peroxide category consists of H_2O_2, hydroxymethylhydroperoxide (and comeasured analogs), and methylhydroperoxide (and comeasured analogs).

sequence high O_3 > mid-O_3 > low O_3 as expected based on solar intensity (Figure 2) and radical precursor concentration (Figures 1a and 1b). The ordering of NO (Figure 1c) also favors O_3 production on high-O_3 days relative to mid- and low-O_3 days. In SOS91, high-O_3 days were predicted to have the greatest O_3 production rate, but the calculations indicated that low-O_3 days produced slightly more O_3 than mid-O_3 days. It is not clear why there are differences between 1991 and 1992, but the role of a less sensitive NO_x detector in 1991 must be considered.

4.2. Photostationary State

Another measure of $dO_3/dt(+)$ is obtained from observed deviations in the photostationary state [*Parrish et al.*, 1986]. The reactions that cycle NO and NO_2 back and forth are

(R9) $$NO_2 + h\nu \rightarrow NO + O(j_{NO_2})$$

(R10) $$O + O_2 \rightarrow O_3$$

(R12) $$NO + O_3 \rightarrow NO_2$$

In addition, NO is converted to NO_2 by (R7) and (R8) leading to net formation of O_3. Assuming (R7)–(R10) and (R12) to be the only relevant processes, we obtain

$$dO_3/dt(+) = j_{NO_2}[NO_2] - k_{12}[NO][O_3] \quad (9)$$

$$[HO_2] + [RO_2] = (j_{NO_2}/k_7)[NO_2]/[NO] - (k_{12}/k_7)[O_3] \quad (10)$$

The total chemical rate of change is defined as in (6) and (7) to include loss due to photolysis and reaction with HO_2,

$$dO_3/dt = dO_3/dt(+) - \text{Loss} \quad (11)$$

where "Loss" has been calculated as in (7), i.e., using an HO_2 concentration calculated from the radical budget equation (3).

NO and NO_2 concentrations needed to evaluate that the PSS relations were obtained from a single channel instrument that switched between NO and NO_2 modes every 5 min. Each pair of adjacent NO and NO_2 determinations was used in the PSS equations along with O_3, temperature, and solar intensity measured at the time midpoint of the NO – NO_2 data points. Thus these measurements are not simultaneous, there being a 5-min difference between NO and NO_2 and a 2.5-min difference between either NO and NO_2 and O_3. To minimize the effects of nonsimultaneous measurements, a screening procedure was employed to discard data points taken under nonstationary conditions. Criteria for acceptable data were that the relative standard deviation of O_3 and solar intensity over a 10-min period preceding the data point in question not exceed 10% and that the value of O_3 and solar intensity at the data point not differ by more

Table 1. Daily Average Radical Production on High-O_3 Days

Source	Amount, ppb	Percent
O_3	11.7	55
HCHO	5.7	27
Other carbonyls	2.9	14
Peroxides	0.9	4
Total	21.2	100

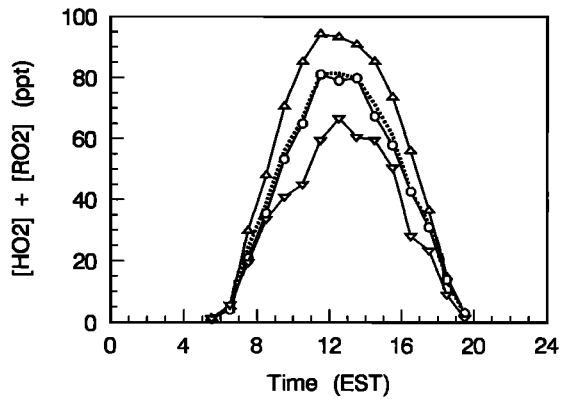

Figure 6. Diurnal cycle for peroxy radical concentration calculated from radical budget (equation (3)) for the whole experimental period and for the high-, mid-, and low-O_3 day subsets. Curve symbols are the same as in Figure 1.

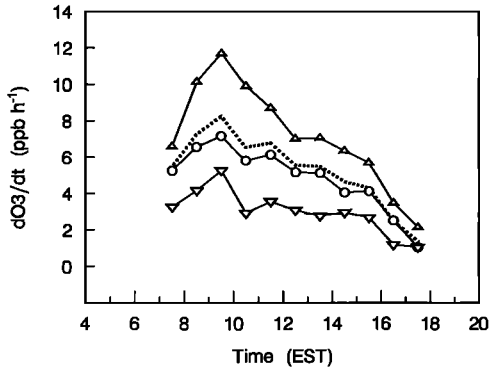

Figure 7. Diurnal cycle for $dO_3/dt(+)$ calculated from radical budget (equation (5)) for the whole experimental period and for the high-, mid-, and low-O_3 day subsets. Curve symbols are the same as in Figure 1.

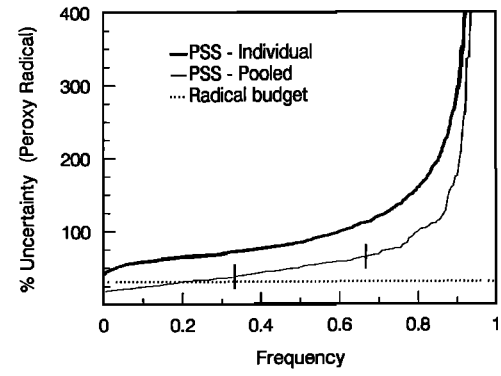

Figure 8. Frequency distribution of estimated fractional uncertainty in peroxy radical concentration calculated from photostationary state (PSS) with a comparison to radical budget result. Uncertainty of hourly average PSS results from equation (12). Plot omits 6% of hourly average distribution with uncertainty greater than 400% and 8% of individual distribution with uncertainty greater than 400%. Hourly average distribution is divided into thirds having low, middle, and high uncertainty.

than 10% from the 10-min average. The period of valid data is restricted by these criteria to be between 0700 and 1800 EST due to large relative changes in solar intensity before and after. Peroxy radical concentration and dO_3/dt were then averaged over valid data points in a 1-hour interval. The screening procedure does not eliminate periods in which NO and NO_2 are rapidly varying due to transport factors and an additional 3 hours of PSS data was deleted where this was the case.

Uncertainties in peroxy radical concentration and $dO_3/dt(+)$ from the PSS relations were estimated based on (8) and the following component uncertainties: $\sigma(NO) = 0.1[NO]$, $\sigma(NO_2) = 0.2[NO_2]$, $\sigma(O_3) = 0.05[O_3]$, and $\sigma(j_{NO_2}) = 0.2j_{NO_2}$. We have applied (8) to each PSS determination. Multiple measurements within a given hour were assumed to be independent of each other and a pooled uncertainty for the hourly averaged PSS determination calculated according to

$$\sigma = (1/N)\left(\sum \sigma_i^2\right)^{1/2} \tag{12}$$

The fractional uncertainty is σ/F, where F is an hourly average value for $[HO_2] + [RO_2]$ or $dO_3/dt(+)$. Equations (9) and (10) give PSS predictions as a difference between two comparable size terms, thereby having the potential of leading to large uncertainties. The fractional uncertainty in peroxy radical concentration, in fact, becomes infinite as peroxy radical concentration approaches zero. The difficulty in basing statistical comparisons on individual PSS determinations because of random variations in NO_x measurements has been previously noted [*Chameides et al.*, 1990]. The averaging procedure in (12) will bring the PSS results into the same time frame as the radical budget results and also remove some of the effects of measurement imprecision.

Estimated fractional errors for the SOS data set are shown in Figure 8 in the form of two frequency distributions pertaining to the individual data points (n = 1103) and to the hourly average determinations (n = 193). In both cases there is an appreciable population of points with uncertainties greater than 100%. The median uncertainty is 51% for the hourly average measurements and 84% for the individual measurements. For comparison, we estimated in the preceding section that the radical budget calculation of peroxy radical concentration had an uncertainty of 31%.

Figure 9 shows two diurnal cycles for the median value of the fractional uncertainty in $[HO_2] + [RO_2]$. One cycle pertains to the individual measurements and the other is the hourly average uncertainty determined from (12). The average number of valid data points per hour varies from about 2 to 9, causing the hourly average uncertainty to be lower than the individual uncertainty by a factor of about 1.4 to 3. Because of the every other hour schedule for calibrating the NO_x detector, the number of valid measurements is greater in odd-number hours, causing a sawtooth appearance to the predicted hourly average uncertainty. There is also a systematic effect whereby the uncertainty increases toward the end of the afternoon. Median values were used in Figure 9 in preference to average values, as the averages are dominated by very high uncertainties occurring when $[HO_2] + [RO_2]$ approaches zero. Results for $dO_3/dt(+)$ are similar.

The peroxy radical concentration and O_3 formation rate calculated from the PSS relations are shown in Figures 10

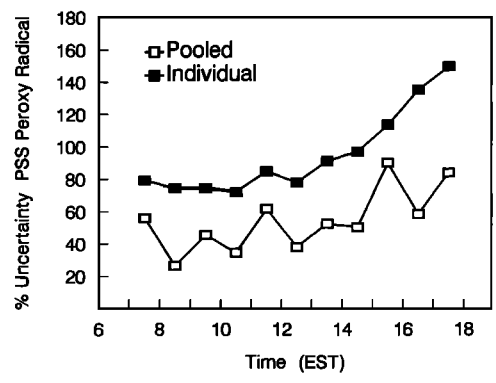

Figure 9. Diurnal cycle of estimated fractional uncertainty in peroxy radical concentration calculated from PSS. Equation (12) is applied to each hour of each day yielding (up to) 28 data points for each hour of the day. The median value of these points is the hourly average or "pooled" curve. The median of the individual data points is determined from the set of all measurements within a given hour.

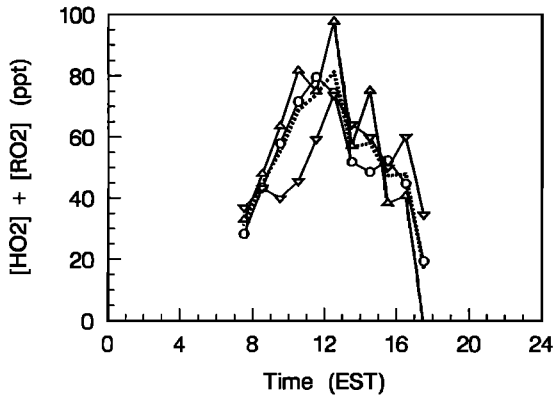

Figure 10. Diurnal cycle for peroxy radical concentration calculated from PSS (equation (10)) for the whole experimental period and for the high-, mid-, and low-O_3 day subsets. Curve symbols are the same as in Figure 1.

and 11, respectively. A quantitative comparison with the corresponding radical budget results is provided in the next section. For now we note that the PSS diurnal cycles are noticeably more "noisy" than their radical budget counterparts (Figures 6 and 7). The clear ordering among high-, mid-, and low-O_3 days is missing, particularly in the afternoon.

4.3. Comparison Between Radical Budget and Photostationary State

Radical budget and PSS expressions for $dO_3/dt(+)$ and peroxy radical concentration depend on different combinations of atmospheric observations. Agreement between these two sets of predictions to the extent permitted by the estimated uncertainties in each would give us confidence in our understanding of the photochemical production of O_3.

Figures 12 and 13 are scatter diagrams showing the relation between hourly average PSS and radical budget predictions for $[HO_2] + [RO_2]$ and $dO_3/dt(+)$. Regression statistics are summarized in Table 2. A visual inspection of Figures 12 and 13 as well as the calculated least squares fits indicates a near 1 to 1 relation between PSS and radical budget calculations. An example of a time series comparison for a single day is given by *Kleinman et al.* [1994b].

The correlation for $dO_3/dt(+)$ is seen to be significantly

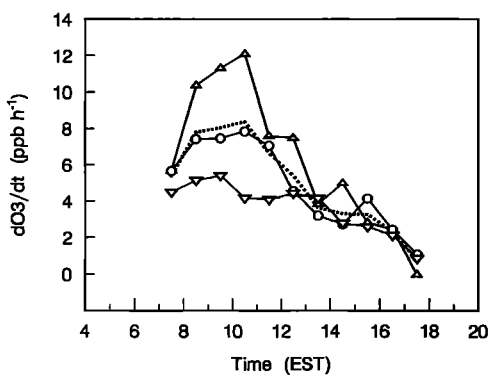

Figure 11. Diurnal cycle for $dO_3/dt(+)$ calculated from PSS (equation (9)) for the whole experimental period and for the high-, mid-, and low-O_3 day subsets. Curve symbols are the same as in Figure 1.

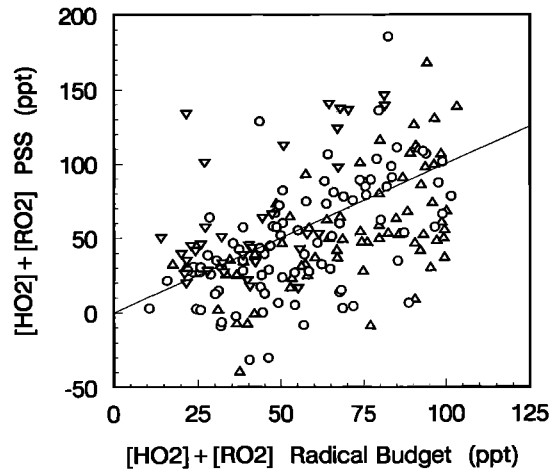

Figure 12. Comparison of hourly average peroxy radical concentration calculated with radical budget and PSS. Curve symbols are the same as in Figure 1. Straight line is 1-to-1 line.

better than that for $[HO_2] + [RO_2]$. This result was not expected in view of (3) and (4) and (9) and (10) which indicate that $dO_3/dt(+)$ and $[HO_2] + [RO_2]$ have the same relation to each other in the PSS and radical budget formulations, i.e., for each 1-hour data point

$$dO_3/dt(+)_{PSS}/dO_3/dt(+)_{RAD} = ([NO]_{PSS}/[NO]_{RAD})\{([HO_2] + [RO_2])_{PSS}/([HO_2] + [RO_2])_{RAD}\} \approx ([HO_2] + [RO_2])_{PSS}/([HO_2] + [RO_2])_{RAD}. \quad (13)$$

An approximately equal sign is used in the above equation because the value for [NO] in the radical budget is a true 1-hour average, while the [NO] used in the PSS equation is an effective average over a portion of an hour with valid data. This difference, however, explains only a fraction of the discrepancy in correlation coefficients. Evidently, there are systematic effects whereby points which contribute the

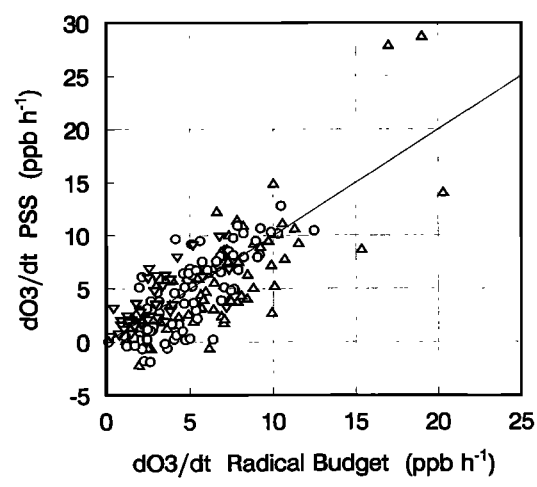

Figure 13. Comparison of hourly average $dO_3/dt(+)$ calculated with radical budget and PSS. Curve symbols are the same as in Figure 1. Straight line is 1-to-1 line.

Table 2. Linear Regression Statistics for Comparison of Photostationary State (PSS) and Radical Budget Predictions of Peroxy Radical Concentration and O_3 Formation Rate

Data Set	Slope[a]	Intercept[a]	r^2
		$[HO_2] + [RO_2]$	
Total	0.82	5 ppt	0.25
High O_3	0.97	−13 ppt	0.35
Mid-O_3	0.99	−7 ppt	0.33
Low O_3	1.40	4 ppt	0.39
		$dO_3/dt(+)$	
Total	0.99	−0.4 ppb h^{-1}	0.60
High O_3	1.13	−2.0 ppb h^{-1}	0.63
Mid-O_3	1.11	−0.9 ppb h^{-1}	0.61
Low O_3	0.94	1.1 ppb h^{-1}	0.49

[a]PSS is equal to intercept plus slope multiplied by radical budget.

most to the correlation coefficient in Figure 13 have similar ratios, close to 1.

Cantrell et al. [1993] examined the frequency distribution of the ratio of peroxy radical concentration determined from the PSS to that measured by a chemical amplifier. We adopt a similar procedure here, using radical budget predictions in place of chemical amplifier measurements in order to quantify the correspondence between PSS and radical budget predictions.

Figure 14 shows the frequency distribution of $([HO_2] + [RO_2])_{PSS}/([HO_2] + [RO_2])_{RAD}$ plotted on a logarithmic scale. According to (13) the distribution for ozone formation rate will be nearly the same. Figure 14 also shows a Gaussian fit to the distribution. As described by Cantrell et al., the width of this Gaussian is a measure of the uncertainty in the ratio, while the distance of the peak from zero is a bias. The fitted Gaussian yields a bias of 13% (PSS values greater than radical budget values) and an uncertainty in the ratio of 62%. Before we compare this uncertainty to that expected, we note that Figure 8 shows that there is a very wide spread in the uncertainties of the hourly PSS determinations. Also, the

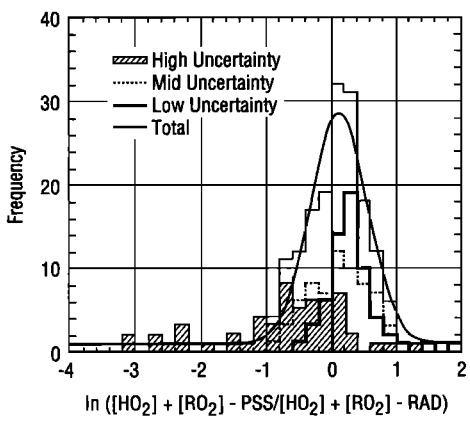

Figure 14. Frequency distribution for the logarithm of the ratio of peroxy radical concentration predicted by the PSS and radical budget equations, i.e., $\ln \{([HO_2] + [RO_2])_{PSS}/([HO_2] + [RO_2])_{RAD}\}$. Hourly averaged values are used. Distributions are shown for the full data set and for the subsets having low, middle, and high uncertainties, as defined in the text. The Gaussian curve is a fit to the total data set.

frequency distribution in Figure 14 seems to contain a population of ratios at low values (below −2) which are outliers to the fitted Gaussian.

The high-uncertainty points interfere with a comparison between PSS and radical budget predictions. One way of preceding is to consider a subset of points with high j_{NO_2}, a cutoff of 0.006 s^{-1} being used by *Parrish et al.* [1986] and *Cantrell et al.* [1993]. These points tend to have low uncertainty and as shown by Cantrell et al., they yield a better agreement with measurements. We have, instead, segregated the data set based directly on the estimated uncertainties. The data set has been split into three equal size subsets according to the PSS uncertainties calculated for each hourly data point. Figure 8 shows that the subset with low uncertainty has a median uncertainty of 28%, those with middle and high uncertainties have median values of 51 and 110%, respectively. A comparison between peroxy radical concentration calculated from PSS and radical budget approaches, applied to the low-uncertainty subset, yields a r^2 correlation of 0.53, a significant reduction in scatter as compared with the data in Figure 12. Gaussian curves have been fit to the low- and mid-uncertainty subsets, with results summarized in Table 3. The high-uncertainty subset which encompasses the previously noted outliers was judged to be not adequately fit by a Gaussian curve.

The expected error in $\ln [([HO_2] + [RO_2])_{PSS}/([HO_2] + [RO_2])_{RAD}]$ is properly calculated from (8), taking into account that some of the same measurements are used in the PSS and radical budget determinations of peroxy radical concentration. Also, we note that uncertainties in rate constants do not contribute to the spread of values of the ratio but only to the bias. For this study we adopt the expedient procedure of estimating the error in the ratio from

$$\sigma_{ratio} = (\sigma_{PSS}^2 + \sigma_{RAD}^{2*})^{1/2} \quad (14)$$

where σ_{PSS} and σ_{RAD}^* are fractional uncertainties of hourly average quantities; σ_{PSS} is taken to be the median value for the data set (i.e., 0.51, 0.28, 0.51, or 1.1 for the total, low-, mid-, or high-uncertainty subsets) and σ_{RAD}^* is calculated as before, except that we ignore the uncertainty in k_6. A value of 0.26 is obtained for σ_{RAD}^*. Results from (14) agree closely with detailed calculations based on (8). Predicted widths of the frequency distributions in Figure 14, determined from (14), are given in Table 3 alongside the widths of the Gaussian fits to these distributions.

Table 3 indicates a reasonable agreement between pre-

Table 3. Comparison of Frequency Distribution of $\ln [([HO_2] + [RO_2])_{PSS}/([HO_2] + [RO_2])_{RAD}]$ to That Expected Based on Uncertainty Analysis

Subset	Bias,[a,b] %	Width of[a] Distribution, %	Calculated Uncertainty,[c] %
Total	13	62	57
Low uncertainty	22	32	38
Middle uncertainty	14	72	57
High uncertainty	−48[d]	···	113

[a]Determined from Gaussian fit to distribution.
[b]Positive bias corresponds to PSS peroxy radical concentration greater than that predicted from radical budget.
[c]Calculated from equation (14).
[d]Median value of distribution.

dicted and estimated uncertainty for the data set as a whole and for the low- and mid-uncertainty subsets. We take this as evidence that our uncertainty estimates are qualitatively correct and that there is indeed a significant difference between low-, mid-, and high-uncertainty subsets. A corollary of this conclusion is that the limiting factor in making a comparison between PSS and radical budget calculations (for the mid- and high-uncertainty subsets) is the precision of the measurements upon which the PSS determination depends. This is consistent with Figure 8 which indicates that estimated errors for the PSS method are greater than that for the radical budget method in the two thirds of the data set with the highest uncertainty.

The bias, as indicated in Table 3, is between 13 and 22% for the data set as a whole and for the low- and mid-uncertainty subsets. A large negative bias occurs in the high-uncertainty subset. These values are probably as low as can be expected given the much larger component uncertainties. For example, a value of α that is systematically low or high will contribute to the bias.

4.4. Assessment of Precision and Accuracy

Differences between error estimates for PSS and radical budget calculations can be traced back to the functional form of the relevant equations (i.e., compare (3) with (10) and (4) with (9)). The difference form for the PSS calculation, i.e., $A - B$, effectively causes experimental precision to be multiplied by the ratio of A to the quantity $A - B$. For measurements in Metter, Georgia, this factor is greater than 2.2 for 75% of the data and greater than 4.5 for 25% of the data. In other locations, different factors will apply. The radical budget approach has the fortunate attribute of placing the least well known quantities under a square root sign, effectively halving the associated errors.

Fundamentally different aspects of the photochemical system are used to arrive at PSS and radical budget formulas. In many ways the PSS approach is a more direct and cleaner way of determining peroxy radical concentration and O_3 formation rate. Rate constants are well known and the only significant assumption on the chemistry is that conversion of NO to NO_2 above that caused by O_3 can be ascribed to peroxy radical reactions (R7) and (R8). Possible contributions due to other chemical processes have been discussed, but persuasive evidence for their occurrence has not been demonstrated [*Parrish et al.*, 1986]. The PSS equations require that the time derivatives of the independent variables be small enough to be ignored. Conditions under which this occurs have been characterized and are not unduly restrictive [*Cantrell et al.*, 1993].

The radical budget approach in contrast requires several assumptions on the atmospheric chemistry, as discussed in SOS91. Principal assumptions are that (1) the production of free radicals is known based on the limited number of precursors that are measured, (2) the removal of radicals due to OH + HO_2 and reaction with NO_x can be ignored relative to combination reactions leading to peroxides, (3) there are no additional radical loss mechanisms such as might involve aerosol surfaces, and (4) the effective rate constant for peroxide formation is known, or equivalently the relative abundance of different peroxy radicals and their combination rate constants are known. Some of these assumptions are particular to the radical budget approach, while others are a reflection of our overall knowledge of ozone photochemistry.

Detailed calculations based on the full set of photochemical equations, such as done by *Cantrell et al.* [1992, 1993], offer advantages as compared with the radical budget approach but at the cost of being more complicated to implement and requiring additional input measurements (principally hydrocarbons). Such calculations provide the fraction of radicals being removed by reactions with NO_x and also provide the speciation of peroxy radicals. We believe that the major improvement to the radical budget approach would be in obtaining a calculated value for α based on actual hydrocarbon measurements. To some extent this is already incorporated in the radical budget calculation in the form of an α derived from detailed calculations based on measurements in a similar forested location [*Trainer et al.*, 1987, 1991]. The error incurred by ignoring radical − NO_x removal reactions is relatively minor in the low NO_x conditions that exist in Metter, Georgia. Even with a "complete" model and a full set of atmospheric measurements of stable compounds, there will still be limitations to our ability to predict O_3 formation due to assumptions on radical − aerosol loss rates and rate constants, in particular for HO_2 + RO_2.

4.5. Comparison Between Calculated and Observed Ozone Changes

Chemistry is only one of several factors that cause O_3 concentrations to vary during the course of a day and from day to day. In SOS91 we examined the contribution of chemical production and loss to the total change in O_3 concentration. Here we adopt a similar approach and compare calculated dO_3/dt with the observed time rate of change of O_3, defined by a finite difference formula. For hour = n, the observed rate of change of O_3 is given by

$$dO_3/dt(n) = (O_3(n + 1) - O_3(n - 1))/2 \text{ hours} \quad (15)$$

Diurnal cycles for the observed hour-to-hour O_3 change are compared in Figure 15 with those calculated from the radical budget and PSS equations (6) and (11). Calculated values for dO_3/dt are approximately 15% lower than the corresponding values for $dO_3/dt(+)$ which takes into account only chemical production. There is reasonable agreement between PSS and radical budget diurnal cycles, a feature that is seen also for $dO_3/dt(+)$; compare Figures 7 and 11.

As noted in SOS91, there are systematic differences between calculated and predicted rates of change of O_3 which are due to the combined effects of vertical motions and deposition. In the morning, O_3 concentrations increase faster than predicted, which we believe is due to entrainment of air from aloft by the growing convective boundary layer. Deposition is also occurring (perhaps at a rapid rate due to the shallowness of the boundary layer early in the morning) and therefore the difference between observed and predicted O_3 change is a lower bound to the amount of entrainment. Even so, it appears that the major fraction of the early morning O_3 increase is due to chemical production. Later in the day, predicted changes in O_3 are greater than observed. We called attention to this occurrence in SOS91 where we noted that the near-surface layer was apparently a strong source region for O_3 after about 1300 EST. This was particularly evident on high-O_3 days in 1991 where O_3 levels were

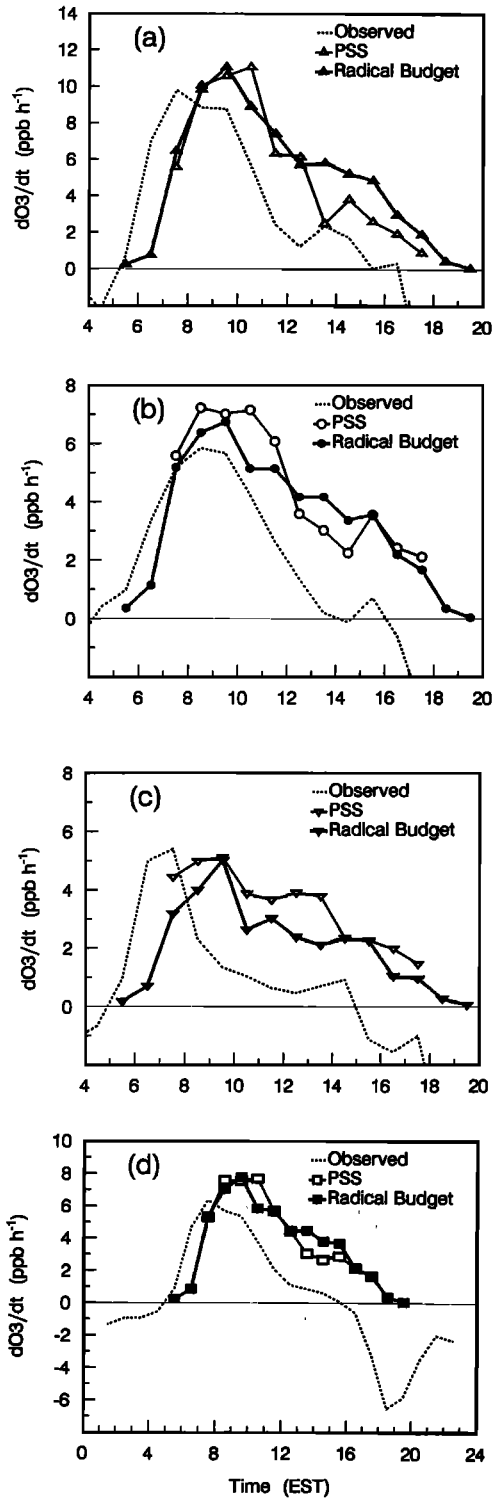

Figure 15. Calculated diurnal cycles for dO_3/dt from radical budget (equation (6)) and PSS (equation (11)) compared with observations (equation (15)) for (a) high-O_3 days, (b) mid-O_3 days, (c) low-O_3 days, and (d) whole experimental period.

observed to decrease even though substantial O_3 production was predicted. In 1992, afternoon O_3 levels increase slightly but not to the extent predicted by the calculations. A possible explanation is that there is dilution of high-O_3 concentration near-surface air due to a continued growth of the boundary layer. Such growth could be the result of fair weather convective clouds [*Lin et al.*, 1994] and/or the result of a step-wise penetration through multiple inversion layers, as observed by *Duncan et al.* [1994]. In order for this mechanism to be effective, O_3 concentrations aloft have to be lower than at the surface, necessitating that O_3 production rates aloft be lower than surface values.

5. Conclusions

Peroxy radical concentration and O_3 formation rate have been determined for the daylight hours of a 28-day SOS measurement campaign in Metter, Georgia, during June 1992. Two methods were used: the photostationary state (PSS) approach and the radical budget approach. These methods depend on different features of the atmospheric photochemical system. Agreement between these methods, to the extent permitted by their respective uncertainties, would indicate a consistent picture of the photochemical production of O_3.

Diurnal cycles of peroxy radical concentration and O_3 formation rate determined by the radical budget approach are in the expected order of highest values occurring on high-O_3 days and lowest values on low-O_3 days. On average, 45% of free radical production is due to precursors other than O_3, primarily HCHO and other carbonyl compounds. The corresponding PSS results are more noisy and are not so clearly ordered.

An uncertainty analysis for the PSS method applied to individual 5-min measurement periods yields a median value of 84% for the estimated fractional uncertainty in peroxy radical concentration. This is reduced to 51% by constructing 1-hour averages. There is an appreciable spread in the uncertainty estimates of the hourly averages which prompted us to split the PSS results into subsets having low, middle, or high uncertainty. Estimated uncertainties for the subsets are 28, 51, and 110%, respectively, as compared with 31% for the radical budget results.

Following *Cantrell et al.* [1993], we have examined the relation between PSS and radical budget predictions by determining the distribution of values in the logarithmic ratio, $\ln [([HO_2] + [RO_2])_{PSS}/([HO_2] + [RO_2])_{RAD}]$. This was done for the data set as a whole and for the subsets defined according to estimated uncertainty. We find reasonable agreement between the spread of values in the ratio and that expected based on uncertainty estimates for the PSS and radical budget methods. There is a small bias with PSS predictions of peroxy radical concentration 13 to 22% greater than radical budget results. PSS and radical budget methods agree to the extent permitted by their respective uncertainties.

Our overall assessment of these two techniques is that the PSS method is more direct and involves fewer assumptions but must be carefully applied due to the difference form of the PSS equations which causes errors to propagate badly. The radical budget method depends on knowing the effective rate constant for peroxy radical combination and upon ignoring radical − NO_x reactions as a sink for free radicals. Error estimates are lower than for the PSS method because the least well known quantities appear under a square root sign.

Comparisons between measured rates of change of O_3 and calculated values from the PSS and radical budget methods

show similar features to that observed during the 1991 SOS campaign (SOS91). Systematic differences are apparent in diurnal cycles averaged over multiday periods because the calculations only take into account chemistry, whereas the evolution of O_3 during the day is affected by the vertical development of the boundary layer and dry deposition. A comparison of observed and predicted diurnal cycles shows the effects of entrainment (and possibly dry deposition) in the early morning. In the middle to late afternoon, O_3 concentration increases at a rate slower than predicted, showing that the near-surface layer is a net exporter of O_3 at that time of the day.

Acknowledgments. The authors appreciate the assistance and cooperation offered by park rangers P. Watson and T. Allmond and their staff at George L. Smith State Park, Georgia. The many contributions of R. Brown, K. Hallock, E. Halper, P. Klotz, and D. Leahy to the success of the SOS field campaign are gratefully appreciated. We would like to thank research groups from the National Center for Atmospheric Research and Georgia Institute of Technology for their participation in the Metter, Georgia, SOS field program. The program for calculating photolysis rate constants was kindly supplied by S. Madronich of NCAR. Part of the support for this study came from the Southern Oxidants Study program with funds principally from the U.S. Environmental Protection Agency. J. Weinstein-Lloyd gratefully acknowledges support of a Department of Energy grant (DE-FG02-91ER61206) and an NSF grant (ATM-9112698). This paper has been authored under contract DE-AC02-76CH00016 with the U.S. Department of Energy under the Atmospheric Chemistry Program within the Office of Health and Environmental Research. Accordingly, the U.S. Government retains a nonexclusive, royalty-free license to publish or reproduce the published form of this contribution or to allow others to do so, for U.S. Government purposes. This research was performed under the auspices of the United States Department of Energy under contract DE-AC02-76CH00016.

References

Aneja, V. P., C. S. Claiborn, Z. Li, and A. Murthy, Exceedances of the National Ambient Air Quality Standard for ozone occurring at a pristine area site, *J. Air Pollut. Waste Manage. Assoc.*, *40*, 217–220, 1990.

Bawkin, P. S., et al., Reactive nitrogen oxides and ozone above a taiga woodland, *J. Geophys. Res.*, *99*, 1927–1936, 1994.

Cantrell, C. A., et al., Peroxy radicals in the ROSE experiment: Measurement and theory, *J. Geophys. Res.*, *97*, 20,671–20,686, 1992.

Cantrell, C. A., et al., Peroxy radicals as measured in ROSE and estimated from photostationary state deviations, *J. Geophys. Res.*, *98*, 18,355–18,366, 1993.

Chameides, W. L., et al., Observed and model-calculated NO_2/NO ratios in tropospheric air sampled during the NASA GTE/CITE 2 field study, *J. Geophys. Res.*, *95*, 10,235–10,247, 1990.

Daum, P. H., L. I. Kleinman, A. J. Hills, A. L. Lazrus, A. C. D. Leslie, K. Busness, and J. Boatman, Measurement and interpretation of concentrations of H_2O_2 and related species in the upper Midwest during summer, *J. Geophys. Res.*, *95*, 9857–9871, 1990.

Davis, D. D., et al., A photostationary state analysis of the NO_2-NO system based on observations from the subtropical/tropical North and South Atlantic, *J. Geophys. Res.*, *98*, 23,501–23,523, 1993.

Duncan, A., A. Stelson, and C. S. Kiang, Estimated contribution of power plants to ambient nitrogen oxides measured on the Georgia Tech. campus in Atlanta, GA: Aug., 1992, *Atmos. Environ.*, in press, 1995.

Kleinman, L. I., Photochemical formation of peroxides in the boundary layer, *J. Geophys. Res.*, *91*, 10,889–10,904, 1986.

Kleinman, L. I., Seasonal dependence of boundary layer peroxide concentration: The low and high NO_x regimes, *J. Geophys. Res.*, *96*, 20,721–20,733, 1991.

Kleinman, L., et al., Ozone formation at a rural site in the southeastern United States, *J. Geophys. Res.*, *99*, 3469–3482, 1994a.

Kleinman, L., et al., Ozone formation at a rural site in Georgia during the summer 1992 SOS campaign, preprint volume, paper presented at the Conference on Atmospheric Chemistry, Am. Meteorol. Soc., pp. 63–67, Jan. 23–28, 1994 Nashville, 1994b.

Lee, J. H., D. F. Leahy, I. N. Tang, and L. Newman, Measurement and speciation of gas phase peroxides in the atmosphere, *J. Geophys. Res.*, *98*, 2911–2915, 1993.

Lee, J. H., I. N. Tang, J. B. Weinstein-Lloyd, and E. B. Halper, An improved nonenzymatic method for the determination of gas phase peroxides, *Environ. Sci. Technol.*, *28*, 1180–1185, 1994.

Lee, Y.-N., and X. Zhou, A method for the determination of some soluble atmospheric carbonyl compounds, *Environ. Sci. Technol.*, *27*, 749–756, 1993.

Lee, Y.-N., X. Zhou, and K. Hallock, Atmospheric carbonyl compounds at a rural southeastern U.S. site, *J. Geophys. Res.*, in press, 1994.

Lin, X., B. A. Ridley, J. Walega, G. F. Hübler, S. A. McKeen, E.-Y. Hsie, M. Trainer, F. C. Fehsenfeld, and S. C. Liu, A parameterization of subgrid scale convective cloud transport in a mesoscale regional chemistry model, *J. Geophys. Res.*, *99*, 25,615–25,630, 1994.

Madronich, S., Photodissociation in the atmosphere, 1, Actinic flux and the effects of ground reflections and clouds, *J. Geophys. Res.*, *92*, 9740–9752, 1987.

McKeen, S. A., E. Y. Hsie, and S. C. Liu, A study of the dependence of rural ozone on ozone precursors in the eastern United States, *J. Geophys. Res.*, *96*, 15,377–15,394, 1991.

Meagher, J. F., N. T. Lee, R. J. Valente, and W. J. Parkhurst, Rural ozone in the southeastern United States, *Atmos. Environ.*, *21*, 605–615, 1987.

National Research Council (NRC), *Rethinking the Ozone Problem in Urban and Regional Air Pollution*, National Academy Press, Washington, D. C., 1991.

Parrish, D. D., M. Trainer, E. J. Williams, D. W. Fahey, G. Hübler, C. S. Eubank, S. C. Liu, P. C. Murphy, D. L. Albritton, and F. C. Fehsenfeld, Measurements of the NO_x–O_3 photostationary state at Niwot Ridge, Colorado, *J. Geophys. Res.*, *91*, 5361–5370, 1986.

Poulida, O., K. L. Civerolo, and R. R. Dickerson, Observations and tropospheric photochemistry in central North Carolina, *J. Geophys. Res.*, *99*, 10,553–10,563, 1994.

Ridley, B. A., S. Madronich, R. B. Chatefield, J. G. Walega, R. E. Shetter, M. A. Carroll, and D. D. Montzka, Measurements and model simulations of the photostationary state during the Mauna Loa Observatory Experiment: Implications for radical concentrations and ozone production and loss rates, *J. Geophys. Res.*, *97*, 10,375–10,388, 1992.

Sillman, S., J. A. Logan, and S. C. Wofsy, The sensitivity of ozone to nitrogen oxides and hydrocarbons in regional ozone episodes, *J. Geophys. Res.*, *95*, 1837–1851, 1990.

Stockwell, W. R., P. Middleton, and J. S. Chang, The second generation regional acid deposition model chemical mechanism for regional air quality modeling, *J. Geophys. Res.*, *95*, 16,343–16,367, 1990.

Trainer, M., E. Y. Hsie, S. A. McKeen, R. Tallamraju, D. D. Parrish, F. C. Fehsenfeld, and S. C. Liu, Impact of natural hydrocarbons on hydroxyl and peroxy radicals at a remote site, *J. Geophys. Res.*, *92*, 11,879–11,894, 1987.

Trainer, M., et al., Observations and modeling of the reactive nitrogen photochemistry at a rural site, *J. Geophys. Res.*, *96*, 3045–3062, 1991.

University Corporation for Atmospheric Research (UCAR), *SERON: The Southeastern Regional Oxidant Network*, Aug. 1990.

L. Kleinman, J. H. Lee, Y.-N. Lee, L. Newman, L. Nunnermacker, S. R. Springston, and X. Zhou, Department of Applied Science, Environmental Chemistry Division, Brookhaven National Laboratory, P.O. Box 5000, Upton, NY 11973-5000.

J. Weinstein-Lloyd, Chemistry/Physics Department, SUNY/Old Westbury, Old Westbury, NY 11568.

(Received June 7, 1994; revised December 19, 1994; accepted December 30, 1994.)